RAPID COMMUNICATIONS

PHYSICAL REVIEW B VOLUME 38, NUMBER 18 15 DECEMBER 1988-II

Calculation of the diamagnetic shift in resonant-tunneling double-barrier GaAs-$Al_xGa_{1-x}As$ heterostructures

Luiz A. Cury,* A. Celeste, and J. C. Portal

Laboratoire de Physique des Solides, Institut National des Sciences Appliquees, F-31077 Toulouse Cedex, France and Service National des Champs Intenses, Centre National de la Recherche Scientifique, F-38042 Grenoble Cedex, France

(Received 7 September 1988)

By using an iteration matrix formalism we calculate the transmission coefficient of $GaAs/Al_xGa_{1-x}As$ double-barrier heterostructures under crossed magnetic and electric fields. A dispersion relation for the total energy of the electron is proposed from which the diamagnetic shift is derived. We extend our calculations to compare with experimental results in a single quantum well [N. J. Pulsford, J. Singleton, R. J. Nicholas, and C. T. B. Foxon, J. Phys. (Paris) Colloq. **48**, C5-231 (1987)]. This method can also be used to compute the transport properties in resonant tunneling devices under a strong magnetic field.

$GaAs/Al_xGa_{1-x}As$ tunneling heterostructures immersed in a magnetic field perpendicular to the growth direction have provided a source of interesting physical problems.[1]

In this paper we treat the problem of a magnetic field perpendicular to the current in a double-barrier resonant-tunneling structure. An applied magnetic field parallel to a two-dimensional electron gas (2D EG) produces a diamagnetic shift of the quantized energy levels. This effect and the cyclotron resonance have been intensively studied in the 2D EG formed at the interface of a heterostructure[2] as well as in single square quantum wells.[3] Our work gives a new way of calculating this diamagnetic shift in quantum wells, based on the transmission coefficient through a double-barrier resonant-tunneling structure in the presence of electric and magnetic fields.

The Hamiltonian for the double barrier under the action of a magnetic field B perpendicular to the electric field F is given by

$$H=(1/2m^*)(\mathbf{p}-e\mathbf{A})^2+V_n(x)-eFx\,, \tag{1}$$

where we have taken the gauge $\mathbf{A}=(0,-Bx,0)$. $V_n(x)$ is the double-barrier square potential.

By using the effective-mass approximation we can write the Schrödinger equation as

$$-(\hbar^2/2m^*)\frac{d^2\psi}{dx^2}+[(m^*\Omega^2/2)(x-x_0)^2+V_n(x)-eF_x]\psi=E\psi\,, \tag{2}$$

in one dimension, where $x_0=-(\hbar K_y/eB)$ and $\Omega=eB/m^*$.

We can obtain an approximate solution by taking the real potential to be a sequential step function, as shown in Fig. 1. This method converges very quickly as it has been demonstrated by Mendez[4] and verified by us. We also consider that the emitter and collector are doped enough to neglect the field effect in these regions. Thus, at each constant potential part we have the Schrödinger equation

$$-(\hbar^2/2m_j^*)\frac{d^2\psi_j}{dx^2}+S_j(x)\psi_j=E\psi_j\,, \tag{3}$$

where $j=0,1,\ldots,M(3)+1$ is the index of each step potential,

$$S_j(x)=\begin{cases}0,\ x<0,\ j=0\,,\\ [U_n(x_{j+1})+U_n(x_j)]/2,\ X_{M(n-1)}<x_j<X_{M(n)},\ [M(n-1)+1]\le j\le M(n)\,,\\ -eFX_{M(3)},\ x>X_{M(3)},\ j=M(3)+1\,,\end{cases} \tag{4}$$

and $n=1,2,3$ is the index of each barrier and well as in Fig. 1. $[M(n)-M(n-1)]$ is the number of steps in each given region n and $X_{M(n)}$ is the position of each interface. The real potential $U_n(x)$ is given by

$$U_n(x)=\begin{cases}-eFx+(m_W^*\Omega^2/2)(x-x_0)^2,\ n\text{ even}\,,\\ U_0=eFx+(m_B^*\Omega^2/2)(x-x_0)^2,\ n\text{ odd}\,,\end{cases} \tag{5}$$

where U_0, m_W^* and m_B^* are, respectively, the potential height of the barrier and the well and barrier effective masses. The general solution for Eq. (3) is given by

$$\psi_j(x)=A_je^{k_jx}+B_je^{-k_jx}\,, \tag{6}$$

where

$$k_j=\begin{cases}i[(2m_j^*/\hbar^2)(E-S_j)]^{1/2},\ E>S_j\,,\\ [(2m_j^*/\hbar^2)(S_j-E)]^{1/2},\ E<S_j\,.\end{cases} \tag{7}$$

By verifying the boundary conditions at each interface, we can find a matrix relation connecting the emitter and collector wave-function coefficients,

$$\begin{pmatrix}A_0\\ B_0\end{pmatrix}=\begin{bmatrix}M(3)\\ \prod_{j=0}L_j\end{bmatrix}\begin{pmatrix}A_{M(3)+1}\\ B_{M(3)+1}\end{pmatrix}\,, \tag{8}$$

where L_j is the iteration matrix given by

$$L_j=\frac{1}{2}\begin{bmatrix}(1+\theta_j)\exp[(k_{j+1}-k_j)x_j] & (1-\theta_j)\exp[-(k_{j+1}+k_j)x_j]\\ (1-\theta_j)\exp[(k_{j+1}+k_j)x_j] & (1+\theta_j)\exp[(k_j-k_{j+1})x_j]\end{bmatrix}, \tag{9}$$

and $\theta_j=(m_j^* k_{j+1}/m_{j+1}^* k_j)$.

By substituting $A_0=1$, $B_0=R$, $A_{m(3)+1}=T$, and $B_{M(3)+1}=0$ we have

$$\begin{bmatrix}1\\ R\end{bmatrix}=\begin{bmatrix}\mathcal{L}_{11} & \mathcal{L}_{12}\\ \mathcal{L}_{21} & \mathcal{L}_{22}\end{bmatrix}\begin{bmatrix}T\\ 0\end{bmatrix} \tag{10}$$

with $\mathcal{L}=\prod_{j=0}^{M(3)} L_j$. R and T are, respectively, the reflection and transmission amplitudes. The transmission coefficient is then given by

$$T^*T(E,K_y,F,B)=(k_{M(3)+1}/k_0)\,|\,1/\mathcal{L}_{11}\,|^2. \tag{11}$$

The numerical results of $\ln(T^*T)$ vs K_y are shown in Fig. 2. For zero magnetic field [Fig. 2(a)] the curve is exactly symmetric. We can see six resonant peaks for an energy $E=0.22$ eV and an electric field $F=0.2\times10^6$ V/m. The other parameters are given in the caption. When the magnetic field is nonzero, the symmetry is lost [Fig. 2(b)]. The numerical results show a displacement in the K_y position of each peak as the magnetic field is increased. We also observe that the distance between each correlated pair of peaks [peaks 1-2, 3-4, and 5-6 in Fig. 2(b)] decreases with increasing B. The amplitudes of each correlated pair of peaks are different, in contrast with the zero-magnetic-field case. To explain these results we propose the following dispersion relation for the total energy of an electron in a double barrier system with applied electric and magnetic field

$$E=E_l^0(F)+(\hbar^2/2m_W^*)(K_y+|K_{0F}(B)|)^2+f_F(B). \tag{12}$$

This relation is schematized in Fig. 3. $E_l^0(F)$ is the lth subband energy in the well when only the electric field is applied. The $E_l^0(F)$ can be found by considering the exact wave function in terms of the Airy functions as done in a previous work.[5] $K_{0F}(B)$ is the shift of the parabola center due to the magnetic field. There is a peak in the transmission coefficient at the values of K_y for which the parabola intersects the total energy E. K_{0F} is then simply given by the average position between the peaks. $f_F(B)$ is the diamagnetic shift. For a zero magnetic field K_{0F} and f_F vanish and we recover the classical dispersion relation $E=E_l^0(F)+(\hbar^2/2m_W^*)K_y^2$.

By comparison of the classical dispersion relation and Eq. (12), for a given total energy and electric field, we can find an expression of the diamagnetic shift

$$f_F(B)=(\hbar^2/2m_W^*)\{K_{pF}^2(B=0)-[\,|K_{0F}(B)|-K_{pF}(B)]^2\}, \tag{13}$$

where K_{pF} is simply given by the peak position in the

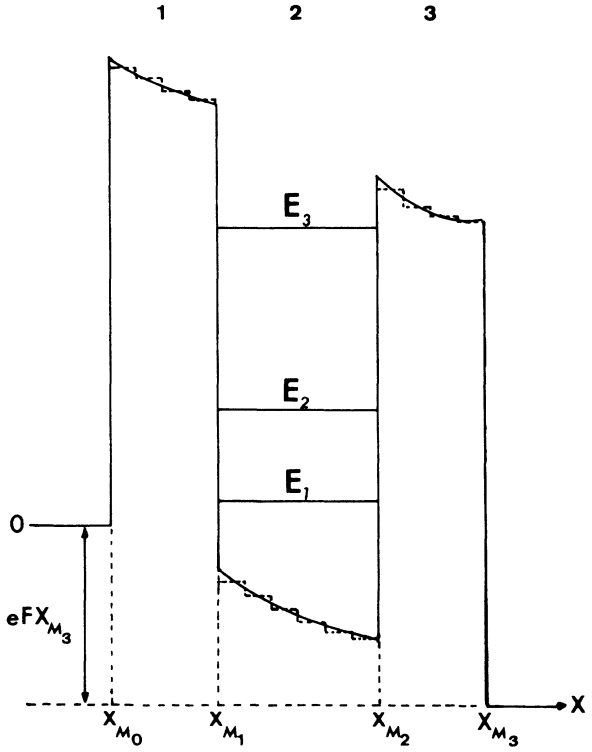

FIG. 1. Double-barrier potential approximated by sequential step functions. The system is under the action of a magnetic field B perpendicular to the electric field F.

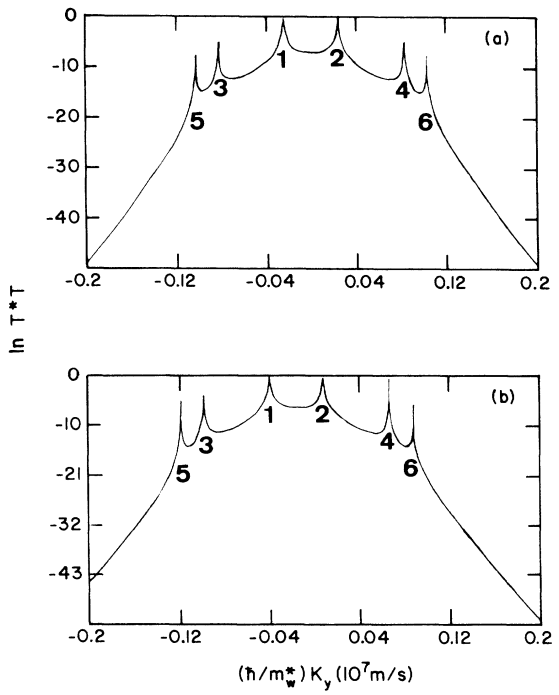

FIG. 2. $\ln T^*T$ vs K_y curve for a $54\times120\times54$ Å^3 $Al_{0.4}Ga_{0.6}As$-GaAs double-barrier heterostructure (a) for zero magnetic field; (b) $B=5$ T. The other parameters are as follows: $F=0.2\times10^6$ V/m, $E=0.22$ eV, $U_0=0.314$ eV, $m_W^*=0.067m_0$, $m_B^*=0.100m_0$, and $x=0.40$.

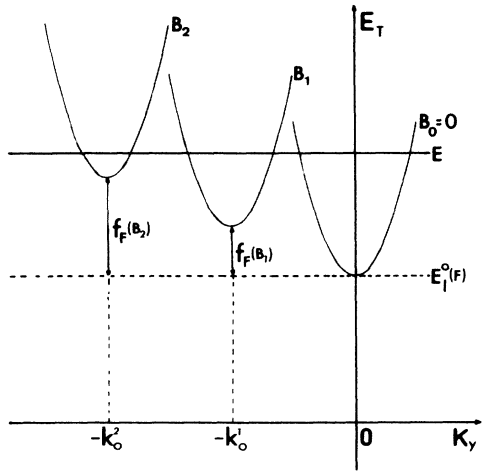

FIG. 3. Scheme of the parabola displacement with increasing of the magnetic field ($B_2 > B_1 > B_0$). $f_F(B)$ is the diamagnetic shift and $K_{0F}(B)$ is the parabola center position.

$\ln(T^*T)$ vs K_y curve, at either sides of $K_0(B)$.

Each correlated pair of peaks is related to an energy subband in the well. Thus, the increase in $f_F(B)$ and $K_{0F}(B)$ with B leads to a change in the positions where the parabola of each subband intersect the total energy E.

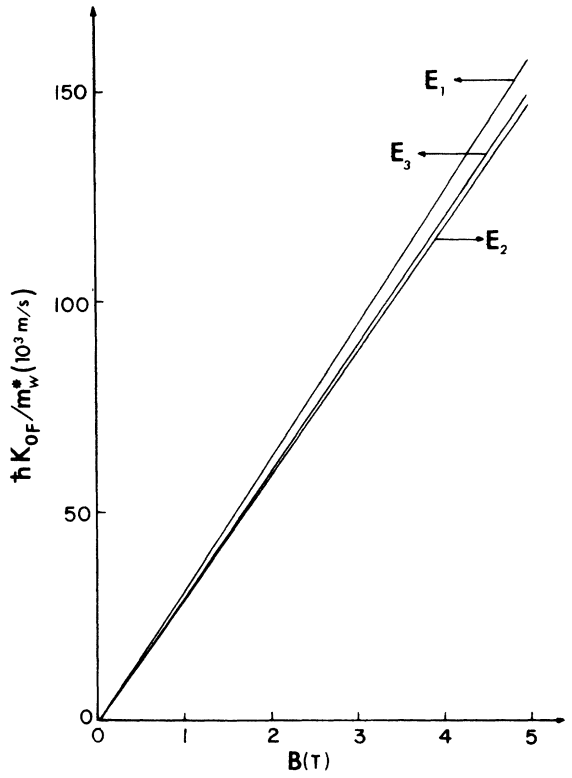

FIG. 4. $K_{0F}(B)$ vs B curve for three different subbands in a 54 Å–120 Å–54 Å double-barrier system in presence of an electric field $F = 0.1 \times 10^7$ V/m. The other parameters are as follows: $U_0 = 0.314$ eV, $m_W^* = 0.067 m_0$, $m_B^* = 0.100 m_0$, and $x = 0.40$.

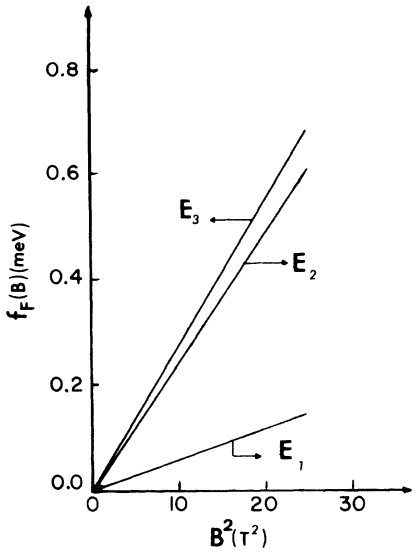

FIG. 5. $f_F(B)$ vs B^2 curve. The double-barrier system and the parameters are the same as those of Fig. 4.

This explains the variation of the peak positions in the $\ln(T^*T)$ vs K_y curve with the magnetic field.

Up to now we have focused on the qualitative results concerning the diamagnetic shift $f_F(B)$ and the displacement $K_{0F}(B)$ of the minimum parabola center. The quantitative results are shown in Figs. 4 and 5. The linear behavior of $K_{0F}(B)$ with the magnetic field and the linear dependence of $f_F(B)$ with the square magnetic field are

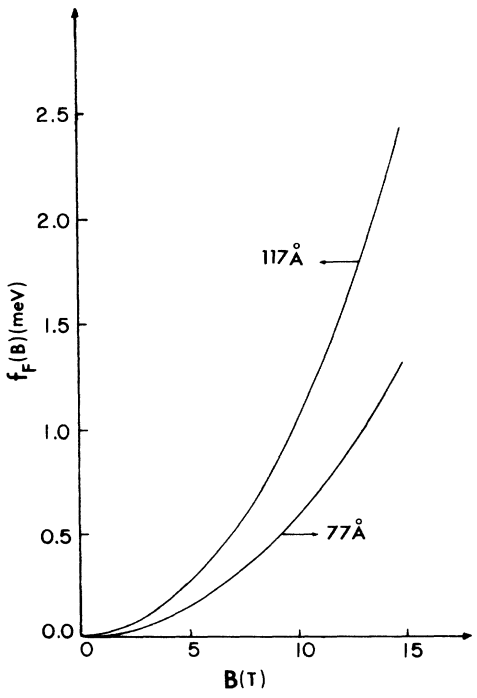

FIG. 6. The numerical first-level diamagnetic shift for two different single-well widths without electric field. The parameters are given in the text.

achieved. These numerical results are in agreement with the perturbational theory contented in Ref. 6. Following these references, the linear coefficients for $K_{0F}(B)$ vs B and $f_F(B)$ vs B^2 curves are given, respectively, by $\alpha_F^l = (e/m_W^*)X_{ll}$ and $\beta_F^l = (e^2/2m_W^*)\,|\,(X^2)_{ll} - (X_{ll})^2\,|$.

X_{ll} and $(X^2)_{ll}$ are expectation values of the respective operators for the unperturbated wave functions and l is the eigenvalue index. In our case, both quantities should be calculated considering the unperturbated system is a double barrier under the action of an electric field. Then for each l subband in the well, the corresponding unperturbated wave function has different behavior. The expectation values X_{ll} and $(X^2)_{ll}$ will be different. This qualitatively explains our results for different slopes, in the $f_F(B)$ and $K_{0F}(B)$ curves, obtained for the three subband energies in the well.

Finally, we have computed the diamagnetic shift for 77- and 117-Å single quantum wells in the absence of electric field to compare with the experimental e_1-hh_1 electron-hole transition performed by Pulsford *et al.*[3] We have considered the wide barrier limit in our model. A systematic study has shown that a barrier width of 100 Å for electrons and 60 Å for holes are enough to isolate the well. Our numerical results for the total diamagnetic shift due to electrons and holes are shown in Fig. 6. We have taken an aluminum concentration $x = 0.36$. The other parameters[7] are $U_0 = 0.296$ eV, $m_W^* = 0.067m_0$, $m_B^* = 0.087m_0$ for electrons (e); $U_0 = 0.1796$ eV, $m_W^* = 0.62m_0$, $m_B^* = 0.67m_0$ for heavy-holes (hh), in the 60:40 band-bending.

At 15 T magnetic field we found the diamagnetic shifts of 2.4 and 1.3 meV, respectively, for 117- and 77-Å single quantum wells in contrast with the 2.1 and 1.2 meV experimental ones. This good agreement demonstrates the viability of our model.

In conclusion we have developed a new formalism to compute numerically the diamagnetic shift in double-barrier tunneling devices and in a single-square-well heterostructure under crossed electric and magnetic fields. The proposed dispersion relation [Eq. (12)] which comprises the displacement $K_{0F}(B)$ of the parabola center and the diamagnetic shift $f_F(B)$ explains the behavior of the $\ln T^* T$ vs K_y curve with increasing magnetic field B. Comparison with the experimental results in a single quantum well[3] in the absence of electric field shows a good agreement which confirms the valuability of our method. We have also obtained the expected linear behavior of $K_{0F}(B)$ and $f_F(B)$ with B and B^2, respectively, for three different subbands in a double-barrier heterostructure in the presence of an electric field. These results agree qualitatively well with the analytic perturbational theory that describes an accumulation layer of electrons at the Si interface.[6]

By utilizing our expression for the transmission coefficient it is possible to derive a current density formula to compute the transport properties by resonant tunneling in a double-barrier device. This will be made in a future work where the J-V and J-B curves will be analyzed.

One of us (L.A.C.) is very grateful to Conselho Nacional de Pesquisa (CNPq), Brasil for financial support. We acknowledge the financial support from Conseil Regional Midi-Pyrenées and European Communities.

*Permanent address: Departamento de Física e Ciência dos Materiais, Instituto de Física e Quimica de São Carlos, Universidade de São Paulo—São Carlos, Caixa Postal 369, 13 560 São Carlos, Sao Paulo, Brazil.

[1]L. Eaves, D. C. Taylor, J. C. Portal, and L. Dmowski, in *Two-Dimensional Systems: Physics and New Devices,* edited by G. Bauer, F. Kuchar, and H. Heinrich, Springer Series in Solid State Sciences, Vol. 67 (Springer, New York, 1986), p. 96; L. Brey, G. Platero, and C. Tejedor (unpublished); J. K. Jain and Steven Kivelson, Phys. Rev. B **37**, 4111 (1988); T. Duffield, R. Bhat, M. Kosa, F. DeRosa, K. M. Rush, and S. J. Allen, Jr., Phys. Rev. Lett. **59**, 2693 (1987).

[2]R. Lassig, in *High Magnetic Fields in Semiconductor Physics,* edited by G. Landwehr, Spring Series in Solid State Sciences, Vol. 71 (Springer, New York, 1986), p. 270; U. Merkt, *ibid.*, p. 256; H. Sigg, C. J. G. M. Langerak, and J. A. A. J. Peremboom, *ibid.*, p. 248; A. Isihara, K. Ebina, L. Smrcka, and H. Havlova, *ibid.*, p. 332.

[3]N. J. Pulsford, J. Singleton, R. J. Nicholas and C. T. B. Foxon, J. Phys. (Paris) Colloq. **48**, C5-231 (1987).

[4]E. E. Mendez, in *Physics and Applications of Quantum Wells and Superlattices,* edited by E. E. Mendez and K. von Klitzing, NATO Advanced Study Institute, Series B Physics (Plenum, New York, 1987), Vol. 170, p. 159.

[5]Luiz A. Cury and Nelson Studart, Superlattices Microstruct. **4**, 245 (1988); **3**, 175 (1987).

[6]W. Beinvogl, Avid Kamgar, and J. F. Koch, Phys. Rev. B **14**, 4274 (1976); Tsuneya Ando, J. Phys. Soc. Jpn. **39**, 411 (1975).

[7]Sadao Adachi, J. Appl. Phys. **58**, 29 (1985); B. El Jani, P. Gibart, J. C. Portal, and R. L. Aulombard, *ibid.* **58**, 3481 (1985).